

The relationship between the X-ray variability and the central black hole mass

Youjun Lu^{1,2*} and Qingjuan Yu^{3†}

¹ Centre for Astrophysics, University of Science and Technology of China, Hefei Anhui 230026, P. R. China.

² National Astronomical Observatories, Chinese Academy of Sciences

³ Princeton University Observatory, Princeton, NJ 08544-1001, USA.

25 October 2018

ABSTRACT

We assembled a sample of Seyfert 1 galaxies, QSOs and Low-Luminosity Active Galactic Nuclei (LLAGNs) observed by ASCA, whose central black hole masses have been measured. We found that the X-ray variability (which is quantified by the “excess variance” σ_{rms}^2) is significantly anti-correlated with the central black hole mass, and there likely exists a linear relationship $\sigma_{\text{rms}}^2 \propto M_{\text{bh}}^{-1}$. It can be interpreted that the short time-scale X-ray variability is caused by some global coherent variations in the X-ray emission region which is scaled by the size of the central black hole. Hence, the central black hole mass is the driving parameter of the previously established relation between X-ray variability and luminosity. Our findings favor the hypothesis that the Narrow Line Seyfert 1 galaxies and QSOs harbor smaller black holes than the broad line objects, and can also easily explain the observational fact that high redshift QSOs have greater variability than local AGNs at a given luminosity. Further investigations are needed to confirm our findings, and a large sample X-ray variability investigation can give constraints on the physical mechanism and evolution of AGNs.

Key words: galaxies: active – galaxies: nuclei – galaxies: Seyfert – X-rays: galaxies.

1 INTRODUCTION

X-ray variability has long been extensively studied for Active Galactic Nuclei (AGN) (see Mushotzky, Done & Pounds (1993) and references therein). In general, the X-ray flux from AGNs exhibits not only long-term variability, but also very rapid variability on time-scales of less than thousands of seconds. This short time-scale variability indicates that X-ray emission most likely originates in the innermost regions of an AGN, and thus can help unravel the basic parameters of the central engine of AGNs (e.g. mass, accretion rate, geometry and radiation mechanisms).

Previous X-ray observations have revealed that the source flux doubling time-scale is significantly correlated with luminosity (Barr & Mushotzky 1986). Using the long time uninterrupted observations of EXOSAT, Lawrence & Papadakis (1993) and Green, McHardy & Lehto (1993) found that the power density spectra (hereafter PDS) of AGNs are consistent with a single form, but the amplitudes are strongly anti-correlated with the X-ray luminosi-

ties. These results have been confirmed by ASCA data. Nandra et al. (1997) first used the “excess variance” to quantify the X-ray variability of AGNs, and found a significant anti-correlation between X-ray variability and luminosity for an ASCA sample of AGNs with predominantly broad emission line objects. Turner et al. (1999) and Leighly (1999) further extended this investigation to the Seyfert 1 galaxies and QSOs with narrow lines (hereafter NLS1), and found that it introduces larger scatter into the established correlation between X-ray variability and luminosity. Moreover, Turner et al. (1999) found a significant correlation between hard X-ray variability and FWHM of H β , and this introduces a connection between the X-ray variability and the “Eigenvector 1” parameters which is proposed to be related with the fundamental parameters of the central engine (Boroson & Green 1992).

Some possible origins of the correlation between the “excess variance” and the luminosity in X-ray band have been discussed by many authors (Lawrence & Papadakis 1993; Bao & Abramowicz 1996; Nandra et al. 1997; Leighly 1999; Abramart & Czerny 2000). The most obvious one might be that the correlation is related to the source size. One might expect that the characteristic time scales or the “excess variance” should scale or relate with the central

* Current Address: Princeton University Observatory, Princeton, NJ 08544-1001, USA; Email: lyj@astro.princeton.edu

† Email: yqj@astro.princeton.edu

black hole mass (Edelson & Nandra 1999). However, the distribution of the other parameters (probably the inclination, the accretion rate and the absorption properties) in the sample can also make the correlation. In fact, Bao & Abramowicz (1996) suggested that the X-ray variability is produced by bright-spots on a rotating accretion disk, and that the correlation is primarily a projection effect. In their model, X-ray variability was enhanced due to the increased relativistic effects with the change of inclination from a face-on to an edge-on disk. However, this model conflicts with the unified model of AGNs in which typical Seyfert 1 galaxies are observed close to face-on. Recently, Abrassart & Czerny (2000) proposed an alternative explanation for the variability of AGNs based on a cloud model of accretion onto a black hole. The small random rearrangement of the cloud distribution can happen on time-scales on the order of $10^2 - 10^6$ s and may lead to relatively high amplitude variability in X-ray based on the large mean covering factor. However, the number of the clouds and the mean covering factor may be determined by the accretion rate and the central black hole mass, and thus the X-ray variability may be related to some fundamental parameters of the central engine in this regime.

Due to the endeavors of the past decade, the pursuing of measuring the central black hole mass in the galaxies nuclei has resulted in fruitful achievements. First, the central massive dark objects—possibly the supermassive black hole—have been measured in the centre of some nearby galaxies based on high spatial resolution observations of stellar dynamics (Kormendy & Richstone 1995; Magorrian et al. 1998). A tight correlation has been found between the central black hole mass and the stellar velocity dispersion which links the inner nuclei with the large scale galactic environment (Ferrarese & Merritt 2000; Gebhardt et al. 2000a). Secondly, reverberation mapping data can give a reliable estimation of the central black hole mass in AGNs (Peterson & Wandel 1998; Wandel, Peterson & Malkan 1999, hereafter WPM; Kaspi et al. 2000, hereafter KSNMGJ), which cannot be determined by the stellar dynamics due to the bright nuclei. The interesting thing is that the relation between the mass of black hole and the bulge gravitational potential also exists in AGNs (Gebhardt et al. 2000b; Nelson 2000). This consistency may further support that the reverberation mapping method is reliable to determine the black hole mass as the stellar dynamics. All these measurements have somewhat distangled the fundamental parameters of the central engine, and allow us to study the relations between the “excess variance” and the fundamental parameters (e.g. the black hole mass and the accretion rate), and thus shed new light on our understanding of the central engine.

In this paper, we investigate the links between the “excess variance” and the fundamental parameters of the central engine, i.e. the central black hole mass. The sample and data reduction are presented in §2; the statistical analysis and results are presented in §3 and discussed in §4; and finally, the conclusions are summarized in §5.

2 SAMPLE AND DATA REDUCTION

The masses of the central black holes for a bunch of Seyferts and QSOs have been measured using reverberation mapping

data (WPM, Ho 1998, and KSNMGJ), based on the assumption that the line-emission material is gravitationally bound and hence has a near-Keplerian velocity dispersion. This assumption is supported by the recent investigation on the Seyfert 1 galaxy NGC5548 which demonstrates that the kinematics of the broad line region is Keplerian (Peterson & Wandel 1999). There are two kinds of methods to estimate a typical velocity and hence the central black hole mass: one is to measure the Full Width at Half Maximum (FWHM) of each line in all spectra and calculate the mean FWHM, the other uses the rms spectrum to compute the FWHM of the lines (WMP and KSNMGJ); the Virial mass is then determined to be $M_{\text{bh}}(\text{mean})$ or/and $M_{\text{bh}}(\text{rms})$ using FWHM(mean) or/and FWHM(rms) together with the time lags of the lines corresponding to the variance of the ionizing continuum (see WPM and KSNMGJ for details).

We searched in the public ASCA archive up to Oct. 1999 for the sample objects of KSNMGJ and Ho (1998) (the objects in WPM sample are included in the KSNMGJ sample), of which the masses of the central black holes have been measured using the reverberation data, and found that 24 objects have been observed by ASCA. Except two objects, PG1411+442 and PG1700+518, which cannot meet the criteria to do the timing analysis (see the following data processing procedures), all the others are listed in table 1 with the measured Virial reverberation mass (both $M_{\text{bh}}(\text{mean})$ and $M_{\text{bh}}(\text{rms})$; KSNMGJ and Ho 1998).

For consistent with the former investigations, we adopted the same method used by Nandra et al. (1997) and Turner et al. (1999) to do the timing analysis and extract the “excess variance” as follows. We used a 256-second time bin for the light curve. We combined the SIS0 and SIS1 data to increase the signal-to-noise ratio and required all time bins to be at least 99% exposed. We required that the time series in our analysis have at least 20 counts per bin and at least 20 bins in the final light curve. The background was not subtracted from the light curves since it has been demonstrated by Turner et al. (1999) and Leighly (1999) that in practice the background is only a small fraction of the photons and it only has a small effects on the value of “excess variance” for light curves with SIS0+SIS1 counts rate greater than 0.5 counts per second. Even for the objects (PG0844+349, PG0953+415 and NGC4579) which have SIS0+SIS1 counts rate less than 0.5 counts per second in our sample, we found that the difference is not large. Finally, we calculated the normalized “excess variance”,

$$\sigma_{\text{rms}}^2 = \frac{1}{N\mu^2} \sum_{i=1}^N [(X_i - \mu)^2 - \sigma_i^2],$$

where X_i with error σ_i is the count rates for the i points of the light curve with total N points, and μ is the mean value of X_i . The error on σ_{rms}^2 is given by $s_D^2/(\mu^2\sqrt{N})$, where

$$s_D^2 = \frac{1}{N-1} \sum_{i=1}^N \{[(X_i - \mu)^2 - \sigma_i^2] - \sigma_{\text{rms}}^2\mu^2\}^2$$

which is only the statistical error. For 16 out of the objects in table 1, of which the “excess variance” for the combined data of two solid-state imaging spectrometers (SISs) have been measured by Turner et al. (1999), we re-calculated the “excess variance” as a check and the values are almost the same as those tabulated in their paper. Therefore, in the

Table 1. Variability properties and the central black hole masses for AGNs: The central black hole masses are adopted from Table 5 in KS NMJG except for those objects labelled with ^a, from which the central black hole mass are adopted from Ho (1998). The “excess variance” are adopted from Turner et al. (1999) except for those objects labelled with ^b, which are measured in this work.

| Name | Sequence | $\sigma_{\text{rms}}^2 (10^{-3})$ | $\frac{M_{\text{bh}}(\text{mean})}{10^7 M_{\odot}}$ | $\frac{M_{\text{bh}}(\text{rms})}{10^7 M_{\odot}}$ |
|-------------------------|----------|-----------------------------------|---|--|
| 3C120 | 71014000 | 2.95±0.71 | 2.3 ^{+1.5} _{-1.1} | 3.0 ^{+1.9} _{-1.4} |
| 3C390.3 | 73082000 | 0.00±0.86 | 34 ⁺¹¹ ₋₁₃ | 37 ⁺¹² ₋₁₄ |
| | 73082010 | 0.00±0.52 | | |
| NGC3227 | 70013000 | 51.7±14.0 | 3.9 ^{+2.1} _{-3.9} | 4.9 ^{+2.6} _{-4.9} |
| | 73068000 | 20.3±4.7 | | |
| AKN120 | 72000000 | 1.31±0.35 | 18.4 ^{+3.9} _{-4.3} | 18.7 ^{+4.0} _{-4.4} |
| MARK335 | 71010000 | 4.86±1.59 | 0.63 ^{+0.23} _{-0.13} | 0.38 ^{+0.14} _{-0.10} |
| Fairall9 | 71027000 | 0.92±0.59 | 8.0 ^{+2.4} _{-4.1} | 8.3 ^{+2.5} _{-4.3} |
| | 73011000 | 0.82±0.45 | | |
| | 73011010 | 0.15±0.34 | | |
| | 73011020 | 1.72±0.75 | | |
| | 73011030 | 0.55±0.77 | | |
| | 73011040 | 2.76±0.79 | | |
| | 73011060 | 1.02±0.57 | | |
| IC4329A | 70005000 | 1.48±0.76 | 0.5 ^{+1.3} _{-1.1} | 0.7 ^{+1.8} _{-1.6} |
| MARK509 | 71013000 | 0.95±0.21 | 5.78 ^{+0.68} _{-0.66} | 9.2 ^{+1.1} _{-1.1} |
| | 74024030 | 0.77±0.45 | | |
| | 74024040 | 0.11±0.28 | | |
| | 74024050 | 0.00±0.12 | | |
| | 74024060 | 0.00±0.30 | | |
| | 74024070 | 0.00±0.30 | | |
| | 74024080 | 0.74±0.37 | | |
| | 74024090 | 0.86±0.55 | | |
| NGC3783 | 71041000 | 7.91±2.20 | 0.94 ^{+0.92} _{-0.84} | 1.10 ^{+1.07} _{-0.98} |
| | 71041010 | 5.33±1.04 | | |
| | 74054000 | 0.92±0.36 | | |
| | 74054010 | 1.75±0.70 | | |
| | 74054020 | 2.91±1.12 | | |
| | 74054030 | 4.13±1.33 | | |
| NGC4051 | 70001000 | 126.0±24.0 | 0.13 ^{+0.13} _{-0.08} | 0.14 ^{+0.15} _{-0.09} |
| | 72001000 | 162.0±22.4 | | |
| NGC4151 | 71019020 | 3.54±1.34 | 1.53 ^{+1.06} _{-0.89} | 1.20 ^{+0.83} _{-0.70} |
| | 71019010 | 6.05±1.23 | | |
| NGC5548 | 70018000 | 5.49±3.00 | 12.3 ^{+2.3} _{-1.8} | 9.4 ^{+1.7} _{-1.4} |
| | 70038000 | 0.50±0.27 | | |
| | 74038010 | 1.57±0.46 | | |
| | 74038020 | 0.89±0.65 | | |
| | 74038030 | 0.26±0.39 | | |
| | 74038040 | 0.15±0.28 | | |
| NGC7469 | 71028030 | 5.30±3.20 | 0.65 ^{+0.64} _{-0.65} | 0.75 ^{+0.74} _{-0.75} |
| MARK279 ^a | 72028000 | 2.80±0.63 | 4.20 | |
| NGC4593 ^a | 71024000 | 21.3±3.45 | 0.81 | |
| NGC3516 ^a | 71007000 | 7.31±1.21 | 2.30 | |
| PG0804+761 ^b | 75058000 | 1.61±0.74 | 18.9 ^{+1.9} _{-1.7} | 16.3 ^{+1.6} _{-1.5} |
| PG0844+349 ^b | 76059000 | 10.5±3.23 | 2.16 ^{+0.90} _{-0.83} | 2.7 ^{+1.1} _{-1.0} |
| PG0953+415 ^b | 75060000 | 0.30±2.90 | 18.4 ^{+2.8} _{-3.4} | 16.4 ^{+2.5} _{-3.0} |
| PG1211+243 ^b | 70025000 | 6.89±2.93 | 4.05 ^{+0.96} _{-1.21} | 2.36 ^{+0.56} _{-0.70} |
| MARK110 ^b | 73091000 | 1.41±0.47 | 0.56 ^{+0.20} _{-0.21} | 0.77 ^{+0.28} _{-0.29} |
| 3C273 ^b | 70023000 | 0.46±0.13 | 55.0 ^{+8.9} _{-7.9} | 23.5 ^{+3.7} _{-3.3} |
| | 10402000 | 1.30±0.25 | | |
| | 12601000 | 0.32±0.11 | | |

Table 2. The variability properties, central black hole masses for LLAGNs.

| Name | Sequence Number | $\sigma_{\text{rms}}^2 (10^{-3})$ | $\frac{M_{\text{bh}}}{10^7 M_{\odot}}$ |
|---------|-----------------|-----------------------------------|--|
| NGC4258 | 60000180 | 0.75 ± 1.95 | 3.60 |
| | 64000000 | 6.41 ± 1.79 | ... |
| | 64000010 | 7.95 ± 1.92 | ... |
| | 64000020 | 5.65 ± 1.83 | ... |
| NGC4579 | 73063000 | 6.10 ± 1.74 | 0.40 |
| M81 | 15000030 | 1.28 ± 0.45 | 0.40 |
| | 15000050 | 4.98 ± 1.55 | ... |
| | 15000120 | 2.03 ± 1.89 | ... |
| | 15000130 | 1.71 ± 2.23 | ... |

present paper, we adopted the values from Turner et al. (1999). For the other six objects, the measured values are also listed in table 1. Note the “excess variance” for PG1211+143 is almost the same as that measured by Leighly (1999) which was measured by a slightly different method. In particular, there are multiple ASCA observations for 3C273, and the observations which can meet the criteria are listed in table 1.

We noticed that Almaini et al. (2000) introduced a more precise maximum likelihood estimator of the “excess variance”, which can be reduced to the form of Nandra et al. (1997) if the measurement errors are almost identical. All the points of any light curve in our sample have approximately the same measurement errors, and thus the maximum likelihood method should give almost an identical value of the “excess variance” with that given in table 1.

Ptak et al. (1998) measured the X-ray variability for a sample of LLAGNs and found that LLAGNs tend to show little or no significant short term variability. For five objects in their sample, M81, NGC3079, NGC4258, NGC4579 and NGC4594, the black holes are identified at the centre of the galaxies (Kormendy & Richstone 1995; Miyoshi et al. 1995; Magorrian et al. 1998). In order to investigate the relations between σ_{rms}^2 and the central black hole mass, we chose them as our sample objects and calculated σ_{rms}^2 of the combined SISs data in 0.5-10keV band using the same criteria. Unfortunately, NGC3079 and NGC4594 do not meet the criteria described above. We threw these two objects out of our sample.[†] The calculated values of σ_{rms}^2 for the others are listed in table 2. Note the fact that the dominant soft components at 0.4-20keV band of LLAGNs, which are probably thermal and not associated with AGNs, may wash out the variability in hard power-law components (Ptak et al. 1998). It means we may underestimate the “excess variability” for those LLAGNs.

[†] However, one may notice that in the above five objects, NGC3079 has the smallest central black hole with mass $1.3 \times 10^6 M_{\odot}$, while NGC4594 has the largest one with mass $6.5 \times 10^8 M_{\odot}$. Using the gas imaging spectrometers (GISs) 2-10keV data, Ptak et al. (1998) measured the “excess variance” for those objects. NGC3079 has the largest σ_{rms}^2 , while NGC4594 has a negative σ_{rms}^2 which shows no significant variability. This is compatible with the relation between the “excess variance” and the black hole mass discussed in the following sections.

3 STATISTICAL ANALYSIS AND RESULTS

Figure 1 show σ_{rms}^2 as a function of the measured mass of the central black hole M_{bh} . For those objects with the masses measured in two ways, $M_{\text{bh}}(\text{rms})$ and $M_{\text{bh}}(\text{mean})$ are used in Figure 1 A and B, respectively. There is clearly a trend that the objects with small central black holes exhibit large variabilities in both plots, although with a large amount of scatter. In fact, a very tight correlation could not be expected because there are considerable uncertainties in both the black hole mass determination and the σ_{rms}^2 measurements. For example, the measured values of σ_{rms}^2 are affected by a lot of factors, such as the length of the observations and the total time spanned of the observations, etc. (see Leighly 1999 for details); we may also underestimate σ_{rms}^2 of LLAGNs using the SISs data in 0.5-10keV band since the thermal soft component LLAGNs in 0.5-2.0keV bandpass may “wash out” some variability. Moreover, significant changes are evidently observed in σ_{rms}^2 among the X-ray observations of a single source, and we used multiple ASCA observations for several objects which were observed frequently. However, it is evident from Figure 1 that LLAGNs and Seyferts/QSOs all follow the same trend, although the luminosities of LLAGNs are much smaller than those of Seyferts and QSOs. If we consider the “wash out” fact for LLAGNs, the correlation should be tighter.

One may notice that NGC3227 deviates from the main trend in Figure 1. This object is unusual by virtue of its very flat soft X-ray spectrum which may be caused by a dusty warm absorber (George et al. 1998; Komassa & Fink 1997). Probably its variability is enhanced by some changes in the absorber. In addition, Schinnerer, Eckart & Tacconi (2000) reported that the enclosed mass in the inner 25 pc of NGC3227 is about $2 \times 10^7 M_{\odot}$ based on a detection of molecular gas at a distance from nucleus of only ~ 15 pc. Although this mass approximately agrees with the Virial mass of $3.9 - 4.9 \times 10^7 M_{\odot}$ measured by using reverberation mapping data with larger uncertainty, it may suggest that the mass of the central black hole is lower than the measured Virial mass. If the central black hole mass of NGC3227 is really lower than the estimated Virial mass (say, by a factor of 2), NGC3227 would join the main trend. Furthermore, we should caution that some systematic error may exist because the adopted masses are measured by different techniques for LLAGNs and Seyfert 1 galaxies/QSOs. This systematic error should not be very large since the measured masses by these two methods follow the same relation with the galaxies

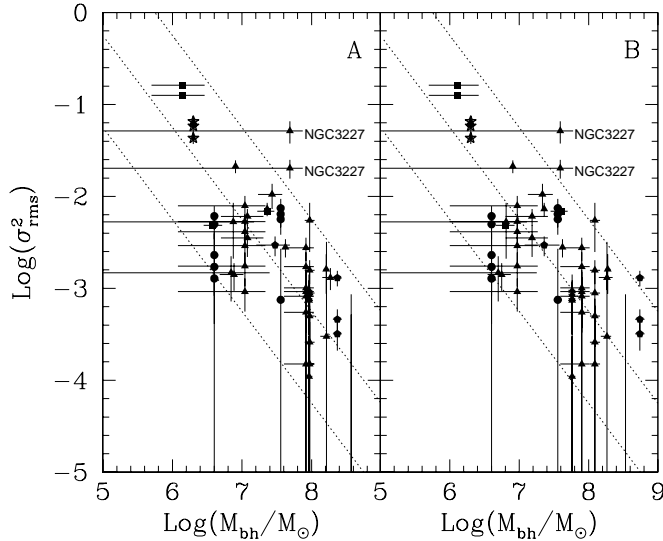


Figure 1. The “excess variance” versus the central black hole mass: $M_{\text{bh}}(\text{rms})$ and $M_{\text{bh}}(\text{mean})$ are used in Figure 1 A and B for those objects which have been measured in two ways. In both plots, the filled triangles represent the radio-quiet Seyfert 1 galaxies and QSOs with broad optical lines; the filled squares represent the Narrow Line Seyfert 1 galaxies and QSOs; the circles represent LLAGNs; the filled pentagons represent the radio-loud objects; and the stars represent MCG-6-30-15, a special object discussed in section 4.

bulge potential (Gebhardt et al. 2000b; Nelson 2000), and the trend still remains even if we exclude those points for LLAGNs in Figure 1.

In Figure 1, the trend seems to be the case that there is a linear relationship, $\sigma_{\text{rms}}^2 \propto M_{\text{bh}}^{-1}$. As we can see, it can be represented by a line $\log \sigma_{\text{rms}}^2 = 4.75 - \log(M_{\text{bh}}/M_{\odot})$ in both Figure 1 A and B. All the objects are localized in the region between the lines $\log \sigma_{\text{rms}}^2 = 3.75 - \log(M_{\text{bh}}/M_{\odot})$ and $\log \sigma_{\text{rms}}^2 = 5.75 - \log(M_{\text{bh}}/M_{\odot})$ except NGC3227. More quantitatively, a Spearman rank test gives the correlation coefficients of -0.70 and -0.65 for the points in Figure 1 A and B, respectively; and rejects the possibility that σ_{rms}^2 and M_{bh} are uncorrelated at $>99.9\%$ confidence. The robust nature of a rank test means that the significance of this correlation does not depend on the outlying point NGC3227. If we include NGC3227 in the test, the corresponding correlation coefficient are -0.68 and -0.64 with almost the same confidence for the points in Figure 1 A and B, respectively.

4 DISCUSSIONS

In the present paper, we found that the “excess variance” is significantly anti-correlated with the central black hole mass for a combined sample of Seyfert 1 galaxies, QSOs and LLAGNs. The most plausible explanation is that the “excess variance” is caused by some global coherent changes in the X-ray emitting region, and this region scales with the size of black hole. The light curves are known to be characterized by a steep power-law PDS ($P(f) \propto f^{-\alpha}$, where $\alpha \sim 1.5 - 2$) in some AGNs, such as NGC4051, NGC3516, NGC5548 and MCG-6-30-15 (Lawrence & Papadakis 1993; Nowak & Chiang 2000). Assuming self sim-

ilar scaling and hence a direct connection between time scales and the size of sources, the observed “excess variance” can be related to the size of the central black hole as $\sigma_{\text{rms}}^2 = \int_{f_1}^{f_2} P(f) df \propto f_1^{1-\alpha} \propto R^{1-\alpha} \propto M_{\text{bh}}^{1-\alpha}$, where $f_1 \ll f_2$ and $\alpha \neq 1$. One can readily get the observed correlation $\sigma_{\text{rms}}^2 \propto M_{\text{bh}}^{-1}$ illustrated in Figure 1 by assuming $\alpha \sim 2$. This fundamental relationship can self-consistently explain the previous finding of the relationship between σ_{rms}^2 and luminosity, which has been proposed by many authors (Nandra et al. 1997; Turner et al. 1999; Leighly 1999; Almaini et al. 2000).

Recently, some investigations have been performed on the relationship between σ_{rms}^2 and luminosity for a sample of LLAGNs (Ptak et al. 1998) and a deep flux limited sample of QSOs selected from deep ROSAT survey (Almaini et al. 2000), which greatly extend the luminosity range and redshift range. Ptak et al. (1998) found that LLAGNs tend to show little or no significant short term variability, and there is a break from the trend of increased variability in Seyfert 1 galaxies with decreased luminosity. They proposed that this is due to the lower accretion rates in LLAGNs. They argued that this results in a larger characteristic size of the X-ray emission region in LLAGNs than in Seyfert 1 galaxies because the lower accretion rate is probably causing the accretion flow to be advection-dominated. However, most of the X-ray emission should originate in an inner volume probably with a radius less than $10R_{\text{Sch}}$ (Ptak et al. 1998), which is similar to the typical X-ray emission region size ($\sim 10R_{\text{Sch}}$) of a normal Seyfert 1 galaxies. If the X-ray variability is caused by some global coherent oscillation for both LLAGNs and normal Seyfert 1 galaxies, then similar variability should be observed in both systems with similar black holes. Indeed, those LLAGNs and AGNs follow the same trend in Figure 1, though LLAGNs have much lower luminosity at a given mass of the central black hole. (However, we should keep in mind that the variability of LLAGNs is possibly fundamentally different from that of normal AGNs.) It can be predicted that many nearby LLAGNs should show little or no significant short term variability because they may harbor “dead” QSOs with larger black holes. This prediction is compatible with the fact that many objects in Ptak et al. (1998) sample show little or no significant short term variability.

Almaini et al. (2000) found that the mean variability of QSOs in a ROSAT sample declines sharply with luminosity as seen in local AGNs, but with an upturn for the most powerful sources. They argued that this is caused by evolution based on the tentative evidence that the high redshift QSOs ($z > 0.5$) do not show the anti-correlation between variability and luminosity as seen in local AGNs. Based on our findings of the direct relation between the variability and the mass of central black hole, a tentative interpretation is that the high redshift QSOs is powered by a less massive black hole and is accreting more efficiently than local AGNs at a given luminosity.

It can be seen in Figure 1 that the several NLS1s (NGC4051, MARK335 and PG1211+143) also follow the same trend with broad line objects. Turner et al. (1999) and Leighly (1999) found that NLS1s have enhanced excess variability at a give luminosity. A simple explanation is that NLS1s have relatively small black holes and enhanced accretion rates. Then the strong correlation between σ_{rms}^2 and

the FWHM of $H\beta$ can be consistently explained (Turner et al. 1999). Furthermore, Mathur (2000) recently argued that NLS1s might be the Seyfert galaxies and QSOs at an early stage of evolution and consequently have small black holes at a given luminosity. He pointed out that they may be low redshift analogues of the high redshift QSOs. This is consistent with the observed fact that the high redshift QSOs have more variability than local AGNs at a given luminosity (Almaini et al. 2000). If the relationship between the variability and the mass of the central black hole is really correct, it is intriguing that a systematic variability study for a large sample (covering a large luminosity and redshift range) can give some information about the accretion history of black holes and some constraints on the evolution scenario of QSOs which has been debated for a long time.

It should be cautioned that the “excess variance” of the NLS1s in our sample is consistent with that of broad line objects rather than the NLS1s on the plot of σ_{rms}^2 versus the luminosity (see Figure 8 in Leighly 1999). One may ask about the other NLS1s. We noticed that MCG-6-30-15 is also a NLS1 with a 1700 km s^{-1} FWHM of $H\beta$ (Turner et al. 1999), and it does show enhanced excess variability on the plot of σ_{rms}^2 versus luminosity (see the Figure 1 in Turner et al. 1999). Nowak & Chiang (2000) recently studied its PDS, and found that the PDS is flat from approximately $10^{-6} - 10^{-5} \text{ Hz}$, and then steepens into a power law $\propto f^{-\alpha}$ with $\alpha \gtrsim 1$ and further steepens to $\alpha \approx 2$ between $10^{-4} - 10^{-3} \text{ Hz}$. Both the PDS shape and rms amplitude are comparable to what has been observed in NGC5548 and CygX-1, though with break frequencies differing by a factor of 10^{-2} and 10^4 . They pointed out that the break frequency may indicate a central black hole mass as low as $10^6 M_\odot$. The monochromatic luminosity at 5100 \AA of this object can be approximately estimated to be $8 \times 10^{42} \text{ ergs s}^{-1}$ (Reynolds et al. 1997), and then its Virial mass can be determined by $M = 1.464 \times 10^5 (R_{\text{BLR}}/\text{lt days})(v_{\text{FWHM}}/10^3 \text{ km s}^{-1})^2 M_\odot \sim 2 \times 10^6 M_\odot$, by using the empirical law $R_{\text{BLR}} = 32.9_{-1.9}^{+2.0} (\lambda L_\lambda(5100 \text{ \AA})/10^{44} \text{ ergs s}^{-1})^{0.700 \pm 0.023} \text{ lt days}$ to estimate the location of broad line region R_{BLR} (KSNMJG). It gives a consistent central black hole mass with the one given by Nowak & Chiang (2000). Furthermore, this value is also consistent with the one given by Reynolds et al. (1995) based on the time scale arguments the 0.5-10keV flux increased by a factor of 1.5 over 100 seconds. We plotted this object in Figure 1, and found that it consistently follows the same trend. Based on above discussion, it is possible true that NLS1s show enhanced excess variation because they harbor smaller central black hole than normal AGNs. However, further systematic investigations are needed to confirm the above interpretation.

Some other models were also proposed to explain the trend of decreasing variability with increasing luminosity. One of them is the multiple independent hot spot model: the variability is caused by independent flaring events, and more luminous systems simply have more flaring regions and hence smaller σ_{rms}^2 . It cannot be simply ruled out since it is plausible that a physical larger emission region will give rise to a greater number of flares (Almaini et al. 2000). However, it is suspected that the flaring mechanism is the same for both the objects with very lower \dot{m} and those with higher \dot{m} . In our sample, \dot{m} must have a broad distribution: the LLAGNs accrete material at a very lower rate and the lu-

minus QSOs may accrete material at high rate. Probably the X-ray emission mechanism for LLAGNs is different from normal Seyfert 1 galaxies and QSOs. For example, the X-ray may be emitted in an inner hot ADAF for LLAGNs, such as M81, NGC4258 and NGC4579 (Gammie, Narayan & Blandford 1999; Quataert et al. 1999), while it is possibly emitted from a corona for normal Seyfert galaxies and QSOs. Another possibility is a toy model of obscurational variability in AGNs, which can also give a relationship between σ_{rms}^2 and the size of central black hole, but in a more complicated way and requiring fine tuning of several parameters, such as the covering factor, the number of the clouds, etc. (see Abrassart & Czerny 2000 for details).

The X-ray spectra of radio-loud objects are generally flatter than those of radio-quiet objects. It is believed that the X-ray is emitted in the jet rather than the disk-corona for radio-loud objects. So, the X-ray variability should be enhanced by relativistic effects. Three radio-loud objects, 3C120, 3C390.3 and 3C373, are included in our sample. However, they do not show significantly enhanced excess variability as shown in Figure 1. This may be caused by that those objects have high inclinations of the disk. Indeed, the best fit of the multi-band spectra of 3C273 give a high inclination of about 60° (Kriss et al. 1999).

There are astrophysical reasons to relate the short-time X-ray variability in AGNs with the accretion rate. For example, high variability can be introduced by some increased instability in high accretion rate objects. However, there are still no reliable estimation for the accretion rate of AGNs. For example, the accretion rate of NGC4258, one of the best studied object, is still in controversy. Its estimated values differ more than one order of magnitude (Neufeld & Maloney 1995; Gammie, Narayan & Blandford 1999). There are separate large amplitude flares in the light curves of many objects, especially in some NLS1 possibly with high accretion rates; what's more, there exists some flare events in the light curves of some NLS1s (e.g. PKS0558-504) which require a very large radiative efficiency (Gliozzi et al. 2000 and references therein). Therefore, the short-time X-ray variability may be more complicated than expected, and it may also depend on some other parameters. A solid conclusion could be drawn by the current broad band X-ray mission like *Chandra* and *XMM-Newton*.

5 CONCLUSIONS

To summarize, we have found a significant anti-correlation between the “excess variance” in X-ray band and the central black hole mass for a composite sample of Seyfert 1 galaxies, QSOs and LLAGNs. Some simple global coherent variations in the X-ray emission region, which scales with the size of the central black hole, can lead to such a relation. Based on our finding, the fact that NLS1 and high redshift QSOs show enhanced excess X-ray variability than broad line local AGNs at a given luminosity can be explained by that they harbor smaller black holes than the normal local AGNs. These results highlight the significance of pursuing a large-sample X-ray variability investigation, which can shed light into the physical mechanism of AGNs and its evolution.

6 ACKNOWLEDGMENTS

We thank an anonymous referee for helpful comments and suggestions and Dr S. P. Oh for a careful reading of the manuscript. YL acknowledges the hospitality of the Department of Astrophysical Sciences, Princeton University. This research has made use of data obtained through the High Energy Astrophysics Science Archive Research Center Online Service, provided by the NASA/Goddard Space Flight Center.

REFERENCES

Brassart, A., Czerny, B., 2000, *A&A*, 356, 475
 Almaini, O., Lawrence, A., Shanks, T., Edge, A., Boyle, B.J., Georgantopoulos, I., Gunn, K.F., Stewart, G.C., Griffiths, R.E. 2000, 315, 525
 Bao, G., Abramowicz, M., 1996, *ApJ*, 465, 646
 Barr, P., Mushotzky, R.F., 1986, *Nature*, 320, 421
 Boroson, T.A., Green, R.F., 1992, *ApJS*, 80, 109
 Edelson, R.A., Nandra, K., 1999, *ApJ*, 514, 682
 Ferrarese, L., Merritt, D., 2000, *ApJ*, 539, L9
 Gammie, C.F., Narayan, R., Blandford, R. 1999, *ApJ*, 516, 177
 Gebhardt, K. et al. 2000a, *ApJ*, 539, L13
 Gebhardt, K. et al. 2000b, *ApJ*, 543, L5
 George, I.M., Mushotzky, R., Turner, T.J., Yaqoob, T., Ptak, A., Nandra, K., Netzer, H., 1998, *ApJ*, 509, 146
 Gliozzi, M., Boller, Th., Brinkmann, W., Brandt, W.N., 2000, *A&A*, 356, L17
 Green, A.R., McHardy, I.M., Lehto, H.J., 1993, *MNRAS*, 265, 664
 Ho, L.C., 1998, In "Observational Evidence for Black Holes in the Universe", ed. S.K. Chakrabarti (Dordrecht: Kluwer) P157
 Kaspi, S., Smith, P.S., Netzer, H., Maoz, D., Jannuzi, B.T., Giveon, U. 2000, *ApJ*, 533, 631 (KSNMJJG)
 Komossa, S., Fink, H., 1997, *A&A*, 327, 483
 Kormendy, J., Richstone, D. 1995, *ARA&A*, 33, 581
 Kriss, G.A., Davidsen, A.F., Zheng, W., Lee, G. 1999, *ApJ*, 527, 683
 Lawrence, A., Papadakis, I.E. 1993, *ApJL*, 414, L85
 Leighly, K.M. 1999, *ApJS*, 125, 297
 Mathur, S., 2000, *MNRAS*, 314, L17
 Magorrian, J., et al. 1998, *AJ*, 115, 2285
 Miyoshi, M., Moran, J., Herrnstein, J., Greenhill, L., Nakai, N., Diamond, P., Inoue, M., 1995, *Nature*, 373, 127
 Mushotzky, R.F., Done, C., Pounds, K.A., 1993, *ARA&A*, 31, 717
 Nandra, K., George, I.M., Mushotzky, R.F., Turner, T.J., Yaqoob, T. 1997, *ApJ*, 476, 70
 Nelson, C. H., 2000, *ApJ*, 544, L9
 Neufeld, D. A., Maloney, P. R., 1995, *ApJ*, 447, L17
 Nowak, M.A., Chiang, J. 2000, *ApJ*, 531, L13
 Peterson, B.M., Wandel, A. 1999, *ApJ*, 521, L95
 Ptak, A., Yaqoob, T., Mushotzky, R., Serlemitsos, P., Griffiths, R. 1998, *ApJL*, 501, 37
 Quataert, E., Di Matteo, T., Narayan, R., Ho, L.C. 1999, *ApJ*, 525, L89
 Reynolds, C.S., Fabian, A.C., Nandra, K., Inoue, H., Kunieda, H., Iwasawa K., 1995, *MNRAS*, 277, 901
 Reynolds, C.S., Ward, M.J., Fabian, A.C., Celotti, A., 1997, *MNRAS*, 291, 403
 Schinnerer, E., Eckart, A., Tacconi, L.J., 2000, *ApJ*, 533, 826
 Turner, T.J., Geroge, I.M., Nandra, K., Turcan, D. 1999, *ApJ*, 524, 667
 Wandel, A., Peterson, B.M., Malkan, M.A., 1999, *ApJ*, 526, 579 (WPM)